

World Journal of *Gastroenterology*

World J Gastroenterol 2023 May 21; 29(19): 2888-3047



REVIEW

- 2888 Radiomics in colorectal cancer patients
Inchingolo R, Maino C, Cannella R, Vernuccio F, Cortese F, Dezio M, Pisani AR, Giandola T, Gatti M, Giannini V, Ippolito D, Faletti R

MINIREVIEWS

- 2905 Branched chain amino acids in hepatic encephalopathy and sarcopenia in liver cirrhosis: Evidence and uncertainties
Marrone G, Serra A, Miele L, Biolato M, Liguori A, Grieco A, Gasbarrini A
- 2916 Assessment of delayed bleeding after endoscopic submucosal dissection of early-stage gastrointestinal tumors in patients receiving direct oral anticoagulants
Sugimoto M, Murata M, Kawai T

ORIGINAL ARTICLE**Basic Study**

- 2932 TATA-box-binding protein-associated factor 15 is a novel biomarker that promotes cell proliferation and migration in gastrointestinal stromal tumor
Guo CM, Tang L, Li X, Huang LY
- 2950 Susceptibility patterns and virulence genotypes of *Helicobacter pylori* affecting eradication therapy outcomes among Egyptian patients with gastroduodenal diseases
Asaad AM, El-Azab G, Abdelsameea E, Elbahr O, Kamal A, Abdel-Samiee M, Abdelfattah A, Abdallah H, Maher D, El-Refaie A, Ghanem SE, Ansari S, Awad SM
- 2961 MMP14 is a diagnostic gene of intrahepatic cholangiocarcinoma associated with immune cell infiltration
Wu J, Guo Y, Zuo ZF, Zhu ZW, Han L

Case Control Study

- 2979 Machine learning model for prediction of low anterior resection syndrome following laparoscopic anterior resection of rectal cancer: A multicenter study
Wang Z, Shao SL, Liu L, Lu QY, Mu L, Qin JC

Retrospective Study

- 2992 Where is the optimal plane to mobilize the anterior rectal wall in female patients undergoing total mesorectal excision?
Jin W, Yang J, Li XY, Wang WC, Meng WJ, Li Y, Liang YC, Zhou YM, Yang XD, Li YY, Li ST
- 3003 Association of vitamin D and polymorphisms of its receptor with antiviral therapy in pregnant women with hepatitis B
Wang R, Zhu X, Zhang X, Liu H, Ji YL, Chen YH

Observational Study

- 3013** Gastrointestinal manifestations of long-term effects after COVID-19 infection in patients with dialysis or kidney transplantation: An observational cohort study

Chancharoenthana W, Kamolratanakul S, Leelahavanichkul A, Ariyanon W, Chinpraditsuk S, Saelim R, Vadcharavivad S, Phumratanaprapin W, Wilairatana P

META-ANALYSIS

- 3027** Short *vs* long-course antibiotic therapy in adults with acute cholangitis: A systematic review, meta-analysis, and evidence quality assessment

Kasparian K, Christou CD, Petidis K, Dumas M, Giouleme O

CASE REPORT

- 3040** Pulmonary hypertension, nephrotic syndrome, and polymyositis due to hepatitis C virus infection: A case report

Zhao YN, Liu GH, Wang C, Zhang YX, Yang P, Yu M

ABOUT COVER

Editorial Board Member of *World Journal of Gastroenterology*, John K Triantafillidis, MD, PhD, FEBGH, Associate Professor of Medicine, Staff Physician, Iasi University of Medicine and Pharmacy, Romania, "Metropolitan General" Hospital, Holargos, Athens 15562, Greece. jktrian@gmail.com

AIMS AND SCOPE

The primary aim of *World Journal of Gastroenterology* (*WJG*, *World J Gastroenterol*) is to provide scholars and readers from various fields of gastroenterology and hepatology with a platform to publish high-quality basic and clinical research articles and communicate their research findings online. *WJG* mainly publishes articles reporting research results and findings obtained in the field of gastroenterology and hepatology and covering a wide range of topics including gastroenterology, hepatology, gastrointestinal endoscopy, gastrointestinal surgery, gastrointestinal oncology, and pediatric gastroenterology.

INDEXING/ABSTRACTING

The *WJG* is now abstracted and indexed in Science Citation Index Expanded (SCIE, also known as SciSearch®), Current Contents/Clinical Medicine, Journal Citation Reports, Index Medicus, MEDLINE, PubMed, PubMed Central, Scopus, Reference Citation Analysis, China National Knowledge Infrastructure, China Science and Technology Journal Database, and Superstar Journals Database. The 2022 edition of Journal Citation Reports® cites the 2021 impact factor (IF) for *WJG* as 5.374; IF without journal self cites: 5.187; 5-year IF: 5.715; Journal Citation Indicator: 0.84; Ranking: 31 among 93 journals in gastroenterology and hepatology; and Quartile category: Q2. The *WJG*'s CiteScore for 2021 is 8.1 and Scopus CiteScore rank 2021: Gastroenterology is 18/149.

RESPONSIBLE EDITORS FOR THIS ISSUE

Production Editor: Yi-Xuan Cai; Production Department Director: Xiang Li; Editorial Office Director: Jia-Ru Fan.

NAME OF JOURNAL

World Journal of Gastroenterology

ISSN

ISSN 1007-9327 (print) ISSN 2219-2840 (online)

LAUNCH DATE

October 1, 1995

FREQUENCY

Weekly

EDITORS-IN-CHIEF

Andrzej S Tarnawski

EDITORIAL BOARD MEMBERS

<http://www.wjgnet.com/1007-9327/editorialboard.htm>

PUBLICATION DATE

May 21, 2023

COPYRIGHT

© 2023 Baishideng Publishing Group Inc

INSTRUCTIONS TO AUTHORS

<https://www.wjgnet.com/bpg/gerinfo/204>

GUIDELINES FOR ETHICS DOCUMENTS

<https://www.wjgnet.com/bpg/GerInfo/287>

GUIDELINES FOR NON-NATIVE SPEAKERS OF ENGLISH

<https://www.wjgnet.com/bpg/gerinfo/240>

PUBLICATION ETHICS

<https://www.wjgnet.com/bpg/GerInfo/288>

PUBLICATION MISCONDUCT

<https://www.wjgnet.com/bpg/gerinfo/208>

ARTICLE PROCESSING CHARGE

<https://www.wjgnet.com/bpg/gerinfo/242>

STEPS FOR SUBMITTING MANUSCRIPTS

<https://www.wjgnet.com/bpg/GerInfo/239>

ONLINE SUBMISSION

<https://www.f6publishing.com>

Basic Study

TATA-box-binding protein-associated factor 15 is a novel biomarker that promotes cell proliferation and migration in gastrointestinal stromal tumor

Cheng-Ming Guo, Li Tang, Xu Li, Liu-Ye Huang

Specialty type: Gastroenterology and hepatology**Provenance and peer review:**

Unsolicited article; Externally peer reviewed.

Peer-review model: Single blind**Peer-review report's scientific quality classification**Grade A (Excellent): 0
Grade B (Very good): B
Grade C (Good): C
Grade D (Fair): 0
Grade E (Poor): 0**P-Reviewer:** Li S, China; Mankotia DS, India**Received:** November 28, 2022**Peer-review started:** November 28, 2022**First decision:** February 15, 2023**Revised:** March 6, 2023**Accepted:** April 11, 2023**Article in press:** April 11, 2023**Published online:** May 21, 2023**Cheng-Ming Guo, Li Tang, Xu Li, Liu-Ye Huang**, Department of Gastroenterology, The Affiliated Yantai Yuhuangding Hospital of Qingdao University, Yantai 264000, Shandong Province, China**Corresponding author:** Liu-Ye Huang, Professor, Academic Research, Chief Doctor, Chief Physician, Research Scientist, Department of Gastroenterology, The Affiliated Yantai Yuhuangding Hospital of Qingdao University, No. 20 Yuhuangding East Road, Yantai 264000, Shandong Province, China. liuye_huang@163.com**Abstract****BACKGROUND**

Gastrointestinal stromal tumor (GIST) is a common neoplasm with high rates of recurrence and metastasis, and its therapeutic efficacy is still not ideal. There is an unmet need to find new molecular therapeutic targets for GIST. TATA-box-binding protein-associated factor 15 (TAF15) contributes to the progress of various tumors, while the role and molecular mechanism of TAF15 in GIST progression are still unknown.

AIM

To explore new molecular therapeutic targets for GIST and understand the biological role and underlying mechanisms of TAF15 in GIST progression.

METHODS

Proteomic analysis was performed to explore the differentially expressed proteins in GIST. Western blotting and immunohistochemical analysis were used to verify the expression level of TAF15 in GIST tissues and cell lines. Cell counting kit-8, colony formation, wound-healing and transwell assay were executed to detect the ability of TAF15 on cell proliferation, migration and invasion. A xenograft mouse model was applied to explore the role of TAF15 in the progression of GIST. Western blotting was used to detect the phosphorylation level and total level of RAF1, MEK and ERK1/2.

RESULTS

A total of 1669 proteins were identified as differentially expressed proteins with 762 upregulated and 907 downregulated in GIST. TAF15 was selected for the further study because of its important role in cell proliferation and migration.

TAF15 was significantly over expressed in GIST tissues and cell lines. Overexpression of TAF15 was associated with larger tumor size and higher risk stage of GIST. TAF15 knockdown significantly inhibited the cell proliferation and migration of GIST *in vitro* and suppressed tumor growth *in vivo*. Moreover, the inhibition of TAF15 expression significantly decreased the phosphorylation level of RAF1, MEK and ERK1/2 in GIST cells and xenograft tissues, while the total RAF1, MEK and ERK1/2 had no significant change.

CONCLUSION

TAF15 is over expressed in GIST tissues and cell lines. Overexpression of TAF15 was associated with a poor prognosis of GIST patients. TAF15 promotes cell proliferation and migration in GIST *via* the activation of the RAF1/MEK/ERK signaling pathway. Thus, TAF15 is expected to be a novel latent molecular biomarker or therapeutic target of GIST.

Key Words: Gastrointestinal stromal tumor; Proteomics; TATA-box-binding protein-associated factor 15; Biomarker; Cell proliferation; Cell migration

©The Author(s) 2023. Published by Baishideng Publishing Group Inc. All rights reserved.

Core Tip: TATA-box-binding protein-associated factor 15 (TAF15) was upregulated in gastrointestinal stromal tumor (GIST) cells and tissues and was associated with a poor prognosis in GIST patients. TAF15 promotes cell proliferation and migration of GIST *in vitro* and tumor growth *in vivo* *via* the activation of the RAF1/MEK/ERK signaling pathway. Therefore, TAF15 is expected to be a novel potential molecular biomarker or therapeutic target of GIST.

Citation: Guo CM, Tang L, Li X, Huang LY. TATA-box-binding protein-associated factor 15 is a novel biomarker that promotes cell proliferation and migration in gastrointestinal stromal tumor. *World J Gastroenterol* 2023; 29(19): 2932-2949

URL: <https://www.wjgnet.com/1007-9327/full/v29/i19/2932.htm>

DOI: <https://dx.doi.org/10.3748/wjg.v29.i19.2932>

INTRODUCTION

Gastrointestinal stromal tumor (GIST) is a common neoplasm that arises from the mesenchymal tissue of the gastrointestinal tract and likely originates from the interstitial cells of Cajal[1,2]. Mutations in mast/stem cell growth factor receptor (KIT) and platelet-derived growth factor receptor A (PDGFRA) are considered the primary causes in the pathogenesis of GIST[3]. GIST most commonly occurs in the stomach (50%-60%) and small intestine (30%-35%) but rarely occurs in the colorectum (5%) and esophagus (< 1%)[4]. Previous studies have indicated that GIST accounts for roughly 0.1%-3.0% of gastrointestinal malignancies, and 15%-50% of patients present with metastasis at the time of diagnosis [5].

In clinical practice, GIST is liable to recur and distantly metastasize even after the initial tumor excision[6]. In fact, about 40% of patients develop tumor metastasis within 15 years after surgery[7], with a strong tendency to metastasize to the liver and peritoneal surfaces primarily and the lymph nodes and lung less frequently[4,8]. Based on tumor size, mitotic count, tumor site, and tumor rupture, the modified National Institutes of Health (NIH) consensus criteria stratifies GIST into four subgroups: Very low (NIH-VL), low (NIH-L), intermediate (NIH-I), and high risk (NIH-H)[9]. GIST patients with large sized tumors and high mitotic counts are more likely to metastasize to the liver and abdominal cavity and frequently have poor disease-free survival ratios[10].

Before the clinical application of imatinib, a tyrosine kinase inhibitor, surgical resection was the only accepted therapy that could prolong the life of GIST patients who had developed metastasis. Even then, the 5-year overall survival rate of patients was only 27%-34%[11]. Improved treatment with imatinib has been highly effective in advanced or metastatic GIST patients, and approximately 80% of them can reach complete or partial recovery[12,13]. Unfortunately, high rates of drug resistance due to secondary mutations of KIT have rendered imatinib therapy ineffective in recent years[14]. Taken together, the current research shows that the therapeutic efficacy of GIST treatments are still not ideal. Therefore, finding new molecular therapeutic targets for GIST is critical.

In this study, we implemented a proteomic analysis in GIST patients using tandem mass tag (TMT) labeling 10-plex kits to explore potential molecular therapeutic targets for GIST. A total of 4111 proteins were quantified in the GIST samples. Of these, 1669 were identified as significant differentially expressed proteins (DEPs), with 762 upregulated and 907 downregulated proteins. After a systematic

analysis of the top 10 upregulated or downregulated proteins, we selected TATA-box-binding protein-associated factor 15 (TAF15) for further study because of its important role in cell proliferation and migration[15]. TAF15 is a member of the FUS/Ewing sarcoma protein (EWS)/TAF15 (FET) family of RNA- and DNA-binding proteins, which plays an essential role in mRNA transcription, RNA splicing and polyadenylation[16-18].

Previous studies have demonstrated that TAF15 can influence a large number of genes that are closely related to the cell cycle and cell death and that overexpression of TAF15 can promote proliferation in sarcomas, human neuroblastoma and leukemia cells[17,19]. TAF15 mediates resistance to radiation therapy through inhibiting tumor suppressors p53 and p21, and upregulation of TAF15 is closely related to worsened survival in non-small cell lung cancer patients[20]. Additionally, a prior study has described a human anti-TAF15 antibody, PAT-BA4, that targeted a tumor-specific TAF15 antigen and then inhibited cell adhesion and spreading in gastric cancer[21]. Moreover, in a recent study, TAF15 activated the mitogen-activated protein kinase (MAPK) signaling pathway by upregulating the expression of MAPK6 in lung squamous cell carcinoma[22]. Taken together, TAF15 may play an important role in the progression of human cancers. However, the latent functions and molecular mechanism of TAF15 in GIST progression are still unclear and must be further studied.

MATERIALS AND METHODS

Clinical sample collection

One hundred and sixty one patients with GIST were recruited from the Department of Gastrointestinal Surgery, Yantai Yu Huang Ding Hospital of Qing Dao University from March 2020 to June 2022, with ethical permission from the Biomedical Ethics Committee (No.2019-410). All patients were diagnosed with GIST by two independent pathologists based on Chinese clinical guidelines[23]. No patients had received chemotherapy before surgery. Out of the 161 cases, 18 cases had matched tumor (T) and normal (N) tissue samples, and the clinicopathologic features of the paired GIST samples were documented in Table 1. In the remaining 143 cases, only tissue from the tumor site was available. In the beginning we only collected 12 matched samples, which were sent for proteomic analysis, followed by another 6 matched samples. All specimens were immediately frozen in liquid nitrogen within 30 min after excision. All patients provided written informed consent.

Protein extraction and digestion

Tissues from GIST patients were homogenized in RIPA lysis buffer containing protease inhibitors using a mortar and pestle. After homogenizing lightly for 1 min on ice, the lysate was centrifuged twice at 13000 RPM for 10 min at 4 °C, and then the supernatants were transferred to a fresh tube. A BCA assay kit (catalog no.P0010, Beyotime Biotechnology, Shanghai, China) was used to measure the protein concentration of each sample. The protein content of each sample was reduced using 5 mmol/L DL-dithiothreitol at 55 °C for 30 min. Samples were then incubated with 10 mmol/L of iodoacetamide at room temperature for 15 min in the dark to alkylate the protein. Each protein sample was dissolved using triethylammonium bicarbonate buffer and then digested overnight at 37 °C using trypsin.

TMT labeling and fractionation

Tryptic peptides from each sample were labeled with TMT (Thermo Fisher Scientific, Waltham, MA, United States) kits following the manufacturer's protocol. After quenching the reaction using 5% hydroxylamine (Sigma-Aldrich, Saint Louis, MO, United States), the TMT-labeled peptide solution was fractionated using basic pH reversed phase high performance liquid chromatography through an Agilent Zorbax Extend C18 column (5 µm, 150 mm × 2.1 mm). The mobile phase consisted of Buffer A (98% water with 2% acetonitrile) and Buffer B (90% acetonitrile with 10% water). The procedure gradient was run as follows: 0%-8% Buffer B for 0-10 min; 8%-35% Buffer B for 10-80 min; 35%-60% Buffer B for 80-95 min; 60%-70% Buffer B for 95-105 min; 70%-100% Buffer B for 105-120 min. The flow rate was set at 1 mL/min. TMT labeled peptides were separated into 10 fractions by reversed phase high performance liquid chromatography.

Liquid chromatography-tandem mass spectrometry analysis

Liquid chromatography-tandem mass spectrometry (MS) analysis was conducted on a Q Exactive Mass Spectrometer (Thermo Scientific) coupled to an EASY-nanoLC System (Thermo Fisher Scientific). Peptides were loaded onto a reverse-phase C18 column (Thermo Scientific Easy Column, 10 cm long, 75 µm inner diameter, 3µm resin) in Buffer A (0.1% formic acid) and separated with a linear gradient of Buffer B (84% acetonitrile and 0.1% formic acid) at a flow rate of 300 nL/min. The MS was utilized in positive ion mode. MS data were acquired following a data-dependent top10 method, dynamically selecting the most abundant precursor ions from the survey scan (300-1800 m/z). The automatic gain control target was set to 3e⁶ with maximum inject time to 10 ms. Survey scans were acquired from a resolution of 70000 at m/z 200 with an isolation width of 2 m/z.

Table 1 Clinicopathologic features of the collected paired gastrointestinal stromal tumors samples

Case No.	Sex	Age in yr	Location	Tumor size length × width × height in cm	Mitosis count, per 50 HFPs	Risk classification based on NIH
1	Male	74	Stomach	2.8 × 2.8 × 2.0	> 5	High
2	Female	24	Stomach	6.0 × 4.0 × 5.0	> 5	High
3	Male	69	Stomach	7.5 × 5.5 × 4.0	> 10	High
4	Male	46	Small intestine	6.5 × 5.0 × 4.0	> 5	High
5	Female	65	Small intestine	6.5 × 5.5 × 5.0	> 5	High
6	Female	61	Stomach	5.5 × 3.5 × 4.0	> 5	High
7	Female	49	Stomach	8.5 × 8.0 × 7.0	< 5	Intermediate
8	Male	77	Stomach	6.0 × 6.0 × 5.0	< 5	Intermediate
9	Female	54	Stomach	6.0 × 4.5 × 3.5	< 5	Intermediate
10	Female	43	Stomach	5.5 × 4.5 × 3.0	< 5	Intermediate
11	Male	70	Stomach	7.0 × 7.0 × 5.5	< 5	Intermediate
12	Female	55	Stomach	8.0 × 8.0 × 7.0	< 5	Intermediate
13	Male	63	Small intestine	5.0 × 3.5 × 3.0	< 5	Low
14	Male	67	Stomach	2.3 × 1.5 × 1.5	< 5	Low
15	Male	44	Stomach	3.0 × 2.7 × 1.3	< 5	Low
16	Female	49	Stomach	1.0 × 0.8 × 0.8	< 5	Very low
17	Female	66	Stomach	2.0 × 1.8 × 1.0	< 5	Very low
18	Female	57	Stomach	2.0 × 1.8 × 1.5	< 5	Very low

HFP: High-powered field; NIH: National Institutes of Health.

Data processing and analysis

Data for each sample were processed using the Swiss-Prot *Homo sapiens* database (20413 entries, January 14, 2017). The parameters of the procedures were as follows: Cysteine carbamidomethylation was set to fixed modification; oxidation was set to variable modification; peptide mass tolerance was 20 ppm, trypsin digestion, max 2 missed cleavages; and the false discovery rate was less than 1%. Proteins with a fold change of > 1.2 or < 0.83 and a *P* value < 0.05 were identified as significantly upregulated or downregulated.

Western blotting analysis

Western blot analysis was performed using 10% sodium dodecyl sulfonate-polyacrylamide gel electrophoresis to separate equal amounts (25 µg/load) of protein samples. Protein samples were transferred onto polyvinylidenedifluoride membranes. The membranes were blocked at room temperature for 1 h with 5% nonfat milk in TBS-T buffer and subsequently incubated with primary antibodies at 4 °C overnight. Secondary antibodies were incubated for 1 hat room temperature. Protein samples were visualized using ECL reagents (MA0186, Meilunbio, Dalian, China) using the ChemiScope 6200 Touch Imaging System (CLINX, Shanghai, China). Some membranes were recycled using stripping buffer (SL1340, Coolaber, Beijing, China) and incubated with other primary antibodies. The primary antibodies were used and obtained as follows: TAF15 (1:3000, ab134916, Abcam, United States); GAPDH (1:5000, D110016, Sangon Biotech, Shanghai, China); RAF1 (1:500, D155090, Sangon Biotech, Shanghai, China); p-RAF1 (1:1000, 66592-1-Ig, Proteintech, Wuhan, China); MEK1/2 (1:1000, 11049-1-AP, Proteintech, Wuhan, China); p-MEK1 (1:1000, 28930-1-AP, Proteintech, Wuhan, China); ERK1/2 (1:1000, 16443-1-AP, Proteintech, Wuhan, China); and p-ERK1/2 (1:1000, 28733-1-AP, Proteintech, Wuhan, China). The secondary antibodies were used and obtained as follows: HRP goat anti-rabbit immunoglobulin G (IgG) (1:3000, D110058, Sangon Biotech, shanghai, China); and HRP goat anti-mouse IgG (1:3000, D110058, Sangon Biotech, Shanghai, China). Three independent tests were performed.

Immunohistochemistry

Tissue specimens were cut into 4 μm sections and processed by deparaffinization and rehydration. Slides were incubated with 3% hydrogen peroxide for 20 min at room temperature to block endogenous peroxidase activity. Tissue sections were incubated with primary antibody TAF15 (1:100, ab134916, Abcam, United States) at 4 °C in a wet chamber overnight and then incubated with secondary antibody HRP goat anti-rabbit IgG (1:100, D110058, Sangon Biotech, Shanghai, China) for 1 h in a wet chamber at room temperature. Color was developed using diaminobenzidine and hematoxylin. Two independent pathologists evaluated the samples by randomly selecting and evaluating five \times 400 microscopic fields per slide. The percentage of stained tumor cells was scored as follows: 0, < 5% positive cells; 1, 5%-24% positive cells; 2, 25%-49% positive cells; 3, 50%-74% positive cells; and 4, \geq 75% positive cells. The staining intensity was scored as follows: 0 for absence; 1 for weak; 2 for moderate; and 3 for strong. The total stained index was equivalent to intensity score \times positive score. A total score \geq 4 was considered positive expression, and < 4 was treated as negative expression.

Cell lines and culture

GIST-882 and GIST-T1 cell lines were obtained from the Shanghai Cancer Institute, and GIST-48 cell lines were kindly provided by Professor Jonathan Fletcher (Harvard Medical School, United States). GIST-882 and GIST-T1 cells were cultured with RPMI 1640 medium (Gibco, United States), and GIST-48 cells were cultured with DMEM (BioInd, Israel). Both medium preparations contained 10% fetal bovine serum (FBS) (Gibco, United States) and 1% penicillin-streptomycin in a humidified incubator at 37 °C with 5% CO₂.

Cell transfection

The lentivirus for knocking down TAF15 (shRNA1, shRNA2, shRNA3) and control scrambled lentivirus (sh-scrambled) were purchased from Genomeditech (Shanghai, China). GIST-882 and GIST-T1 cells were seeded in a 12-well plate (Corning Life Sciences) at 1×10^5 cells per well, and the transfection was performed when the cell density reached about 50%. Cells were cultured in fresh medium after being infected with lentivirus for 72 h. The multiplicity of infection of lentivirus to GIST-882 and GIST-T1 was 30. Stable cell lines were generated through selection with puromycin (2 $\mu\text{g}/\text{mL}$). Transfection efficiency was detected using western blot analysis.

Cell immunofluorescence

Transfected cells were cultured in 12-well plates. When the cell density reached 50%-65%, cells were fixed using 4% paraformaldehyde for 30 min to make slides. 0.5% Triton X-100 was added to slides to allow for cell penetration, and 10% goat serum was used to block cells for 2 h at room temperature. Slides were then incubated with the TAF15 primary antibody (1:500, ab134916, Abcam, United States) at 4 °C overnight and then incubated with secondary antibodies for 1 h at room temperature. DAPI was used to stain the cell nuclei, and images were photographed using a fluorescent microscope. The fluorescent intensity of cells were measured using Image J software (version 3.2.0.8).

Cell counting kit-8 assay and colony formation assay

The cell counting kit (CCK)-8 (Dojindo, Tokyo, Japan) assay was performed according to the manufacturer's instructions. Briefly, different groups of cells were seeded onto 96-well plates at 1×10^3 cells per well. The CCK-8 reagent was added (10 $\mu\text{L}/\text{well}$) into the individual wells during the last hour. A microplate reader (Bio-Rad) was used to measure the optical density of the samples at 450 nm, as a measure of cell proliferation. With respect to the colony formation assay, different groups of cells were cultured in 6-well plates (500 cells/well) for 2 wk. Cell colonies were fixed with 4% paraformaldehyde for 30 min and stained with 1% crystal violet for 15 min at the room temperature. Colonies consisting of 50 or more cells were counted.

Transwell experiment

GIST-882 and GIST-T1 cells (3×10^4 cells/well) were inoculated into the upper polycarbonate membrane chambers of a 12-well plate without FBS, while the lower chamber contained RPMI 1640 medium with 10% FBS. To detect the cell invasion ability, matrix gel was in advance added to the polycarbonate membrane chambers. After being cultured for 48 h, the cells attached to the lower side were fixed with 4% paraformaldehyde for 30 min and stained with 1% crystal violet for 15 min at the room temperature. Five fields were selected randomly to count using an inverted microscope.

Wound healing assay

GIST-882 and GIST-T1 cells were cultured up to 90% confluency and then serum-starved for 12 h. The cell monolayer was scratched using a 1 mL plastic pipette tip. Culture medium was used to wash away the cell debris twice, and then cells were incubated in respective culture medium containing 10% FBS. Samples were photographed at 0 h, 12 h and 24 h post scratch using an Olympus microscope. The percentage of wound healing was evaluated using Image J software.

Modeling of GIST xenografts in nude mice

Nude mice aged 4 wk were purchased from the Beijing Vital River Laboratory Animal Technology Co., Ltd (Beijing, China). All animal care and processing were performed according to the Institutional Animal Care and Use Committee of Qingdao University guidelines. Twenty mice were divided randomly into two groups (10 mice per group) and then subcutaneously injected in the axillary region with stable cells (2×10^6 cells) transfected with sh-TAF15 or sh-scrambled. The volume (volume = length \times width \times width/2) of tumors were measured every 2 d. The mice were humanely sacrificed using the cervical dislocation method after anesthesia with 0.7% sodium pentobarbital. Tumor tissues were then excised, photographed and weighed.

Statistical analysis

Statistical analyses were performed using GraphPad Prism 9.3.1. The data analyses were conducted using Student's *t*-test, χ^2 test, one-way analysis of variance or Mann-Whitney *U* test. Data were expressed as mean \pm standard deviation. *P* < 0.05 was considered statistically significant, and significance was indicated in each graph.

RESULTS

Quantification of DEPs by TMT

In total, 4111 proteins were quantified with a false discovery rate < 0.01 in all 12 GIST matched samples. Of these, 1669 were identified as significant DEPs on the basis of the filtering criteria of fold change > 1.2 or < 0.83 and *P* value < 0.05, including 762 upregulated proteins and 907 downregulated proteins (Figure 1A and Supplementary Table 1). Notably, the key proteins used for diagnosing GIST, including KIT, DOG1 and hematopoietic progenitor cell antigen CD34 (CD34), were all contained in the upregulated protein category (Supplementary Table 1), suggesting that our proteomic data were reliable. Moreover, 667, 686, 840 and 974 significant DEPs were identified in the NIH-H, NIH-I, NIH-L and NIH-VL subgroups, respectively (Figure 1B and Supplemental Table 2). After our systematic analysis of the top 10 upregulated and downregulated proteins (Table 2), we decided to focus on the protein TAF15 due to its important role in cell proliferation and migration.

Identification of TAF15 by western blotting analysis

Western blotting was used to further identify the expression levels of TAF15 in GIST. We detected the extracted proteins from tumor tissues (T) and matched normal tissues (N) of 18 GIST patients, including 6 NIH-H, 6 NIH-I, 3 NIH-L, and 3 NIH-VL cases. The results showed that the expression levels of TAF15 were significantly increased in tumor tissues compared with matched normal tissues (Figure 1C and D), which were in agreement with the results of our quantitative proteomics analysis (Table 2 and Supplemental Table 2).

Validation of TAF15 expression by immunohistochemical analysis

We evaluated the expression level of TAF15 in GIST patients using immunohistochemical (IHC) analysis of tumor tissues (T) from 161 patients and 18 matched normal tissues (N). We found significantly higher levels of expression of TAF15 in tumor tissues compared to matched normal tissues (red arrows, Figure 1E and F, Supplemental Table 3). Moreover, subgroup analyses showed that the expression level of TAF15 was significantly higher in the NIH-H subgroup than in the NIH-I, NIH-L and NIH-VL subgroups and that the expression level of TAF15 was significantly higher in the NIH-I subgroup than the NIH-VL subgroup (Figure 1G and Supplemental Table 3). We found no significant difference in the expression of TAF15 between the NIH-L and NIH-VL subgroups and between the NIH-I and NIH-L subgroups. Furthermore, based on our IHC data, we found that the overexpression level of TAF15 was positively correlated with tumor size and GIST risk stage but was not significantly correlated with gender, age or tumor metastasis (Table 3). These results provided evidence that the higher expression of TAF15 may contribute to malignant progression of GIST and that TAF15 may be a latent promoter or biomarker of GIST.

Knockdown of TAF15 inhibited the proliferation and migration of GIST cells

In order to understand the real role of TAF15 in GIST progression, short-hairpin RNAs (shRNAs) were used to knock down TAF15 in GIST-882 and GIST-T1 cells. GIST-882 and GIST-T1 cells were used instead of GIST-48 cells, as the expression level of TAF15 was higher in the former cell lines (Figure 2A). Three shRNAs targeting TAF15 (sh1, sh2 and sh3) were applied to knock down TAF15 protein. The results showed that sh2 and sh3 could significantly reduce the expression of TAF15 when compared to scrambled shRNA (scr), as tested by western blotting analysis (Figure 2B and C) and cell immunofluorescence assays (Figure 2D and E). Therefore, sh2 and sh3 were used to perform further experiments.

Table 2 The top 10 upregulated and downregulated proteins

Category	Accession	Protein name	FC,T vs N	P value
Up	P29400	COL4A5	3.129881192	0.001086699
	O94772	LY6H	2.995133385	0.012292301
	P05204	HMGN2	2.92528705	2.10765E-07
	O00479	HMGN4	2.900071252	3.22924E-09
	P20930	FLG	2.87152332	0.002555182
	P52926	HMGA2	2.687785701	0.008942412
	Q6UX72	B3GNT9	2.576105848	4.91404E-09
	Q92804	TAF15	2.456058544	1.54458E-05
	O95081	AGFG2	2.441304592	2.93054E-06
	P09936	UCHL1	2.157884674	7.498E-07
Down	Q96BQ1	FAM3D	0.225135868	0.022611851
	Q5DID0	UMODL1	0.242287446	0.00020958
	P25815	S100P	0.267045455	3.77116E-06
	P13640	MT1G	0.274242	0.0028833
	P42330	AKR1C3	0.290893518	6.40059E-07
	Q9UBU3	GHRL	0.293081189	0.000379102
	Q9NS71	GKN1	0.311488849	6.5931E-06
	O95994	AGR2	0.330784665	9.59846E-06
	P19075	TSPAN8	0.350779233	7.40703E-09
	P55087	AQP4	0.352590936	0.035544439

T: Tumor tissues; N: Matched tumor normal tissues; FC: Fold change.

The results of the CCK-8 assay and the colony formation assay indicated that TAF15 knockdown (sh2 and sh3) exhibited a significant decrease in proliferative and colony forming ability in GIST-882 and GIST-T1 cells when compared with the scr (Figure 3A-D). Transwell assay showed that the sh-TAF15 group (sh2 and sh3) exhibited significantly weaker migratory abilities compared to the scr in GIST-882 and GIST-T1 cells (Figure 3E and F). However, there was no significant difference in the invasion ability of GIST-882 and GIST-T1 cells between the sh-TAF15 group (sh2 and sh3) and sh-scrambled group (Figure 3G and H). The results of the wound healing assay also showed that migratory abilities significantly decreased in the sh-TAF15 group (sh2 and sh3) compared to the scr in GIST-882 and GIST-T1 cells (Figure 3I-K). These findings indicated that TAF15 knockdown can significantly inhibit GIST cell proliferation and migration.

TAF15 promoted GIST progression by activating the RAF1/MEK/ERK signaling pathway

Previous studies have shown that EWS, one of the members of the FET family proteins, forms a fusion oncoprotein EWS-FLI1 whose expression leads to the activation of ERK1/2 signaling in zebrafish embryos and adult tumors[24]. In consideration of the important role of the ERK signaling pathway in many human tumors[25], we speculated that TAF15 could promote cell proliferation and migration directly through the activation of the ERK signaling pathway in GIST. Therefore, we assessed the phosphorylation level of RAF1, MEK and ERK1/2 in GIST-882 and GIST-T1 by western blotting. The results showed that the phosphorylation levels of RAF1, MEK and ERK1/2 were significantly decreased following TAF15 knockdown (sh2 and sh3). However, there was no significant change in levels of total RAF1, MEK and ERK1/2 (Figure 4). Collectively, these findings suggest that TAF15 may promote cell proliferation and migration through the activation of the RAF1/MEK/ERK signaling pathway in GIST.

TAF15 promoted the growth of GIST in vivo

To further confirm the role of TAF15 in the progression of GIST, we established a xenograft mouse model utilizing GIST-882 cells due to their enhanced proliferative and migratory ability. sh2 was used in this experiment because of its higher knockdown efficiency, with scr as a control. Twenty nude female mice were randomly divided into two groups, and each mouse was then subcutaneously injected with

Table 3 Correlation between the expression of TATA-box-binding protein-associated factor 15 and clinicopathological characteristics in gastrointestinal stromal tumors

Characteristics	TAF15 expression		P value
	Negative	Positive	
Total number	31	130	
Sex			0.2730 ^a
Male	16 (9.9)	53 (32.9)	
Female	15 (9.3)	77 (58.7)	
Age in yr			0.8228 ^a
≤ 60	15 (9.3)	60 (37.2)	
> 60	16 (9.9)	70 (43.5)	
Tumor size			
Maximum diameter in cm			
≤ 5	29 (18.0)	74 (46.0)	0.0001 ^a
> 5	2 (1.2)	56 (34.8)	
GIST risk stage			0.0021 ^b
Very low risk	15 (9.3)	30 (18.6)	
Low risk	11 (6.8)	31 (19.3)	
Intermediate risk	3 (1.9)	29 (18.0)	
High risk	2 (1.2)	40 (24.8)	
Metastasis			0.1316 ^a
-	31 (19.3)	121 (75.2)	
+	0 (0.0)	9 (5.6)	

^aP values were calculated by χ^2 test.

^bP values were calculated by Mann-Whitney U test.

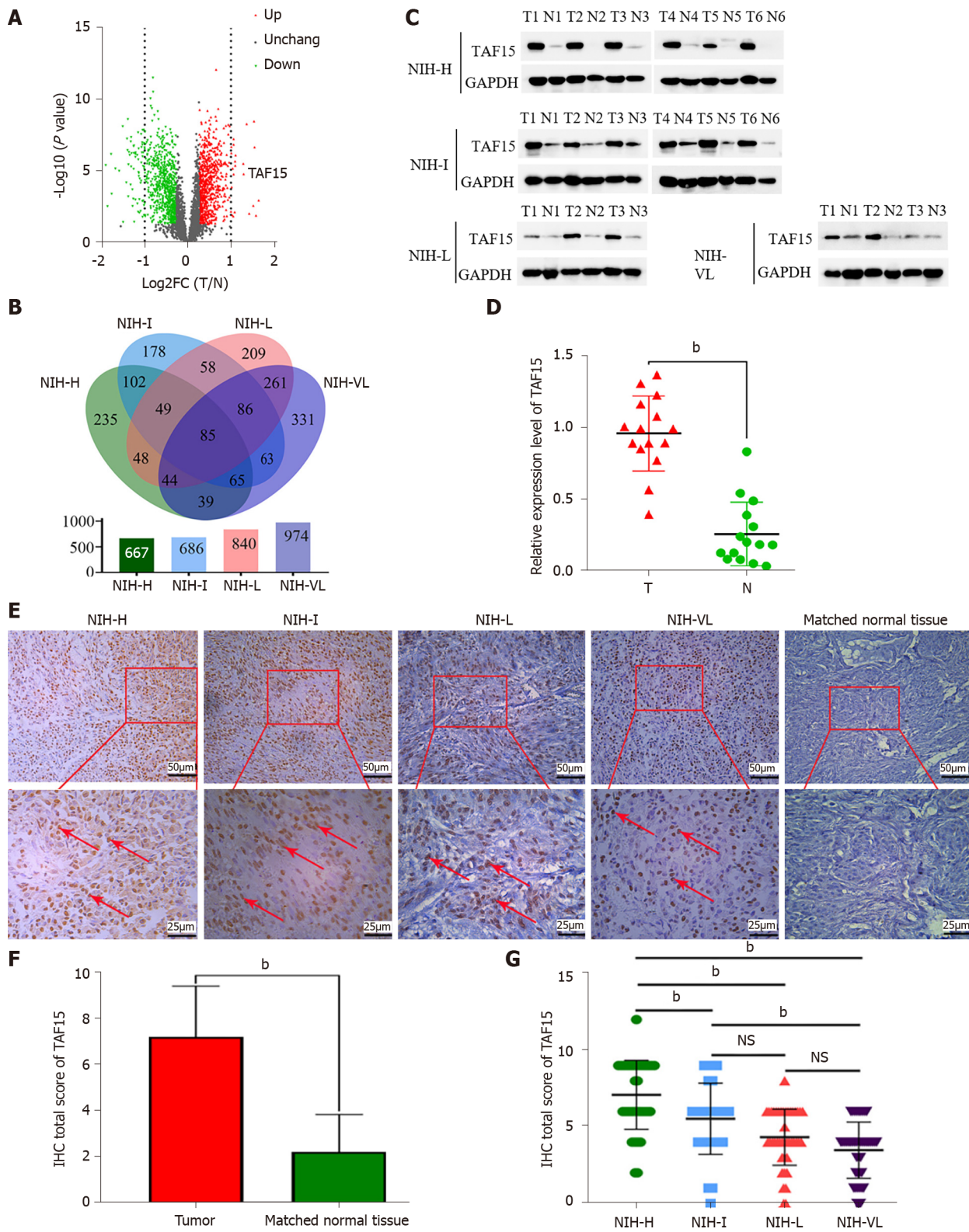
Total patients of 161. Data are presented as *n*(%). TAF15: TATA-box-binding protein-associated factor 15; GIST: Gastrointestinal stromal tumor.

either sh2 or scr cells. Unfortunately, one mouse in the scr group died on day 7 post-injection for an unknown reason. Ten days after injection, xenograft tumors in the remaining mice were detectable. The results showed that TAF15 knockdown significantly suppressed tumor growth and tumor weight (Figure 5A-C). Furthermore, western blotting analysis was used to confirm the level of TAF15 in the xenograft tumors. The results showed that the levels of TAF15 were significantly decreased in the sh2 group compared to the scr group (Figure 5D and E). Additionally, three xenograft tumors of the sh2 group and three xenograft tumors of the scr group were randomly selected to test the levels of RAF1, MEK and ERK1/2 by western blotting. The results indicated that the phosphorylation levels of RAF1, MEK and ERK also decreased significantly in the sh2 group, while the levels of total RAF1, MEK and ERK showed no significant change (Figure 5F-I). These data indicated that TAF15 may promote the growth of GIST *in vivo* via the activation of the RAF1/MEK/ERK signaling pathway.

DISCUSSION

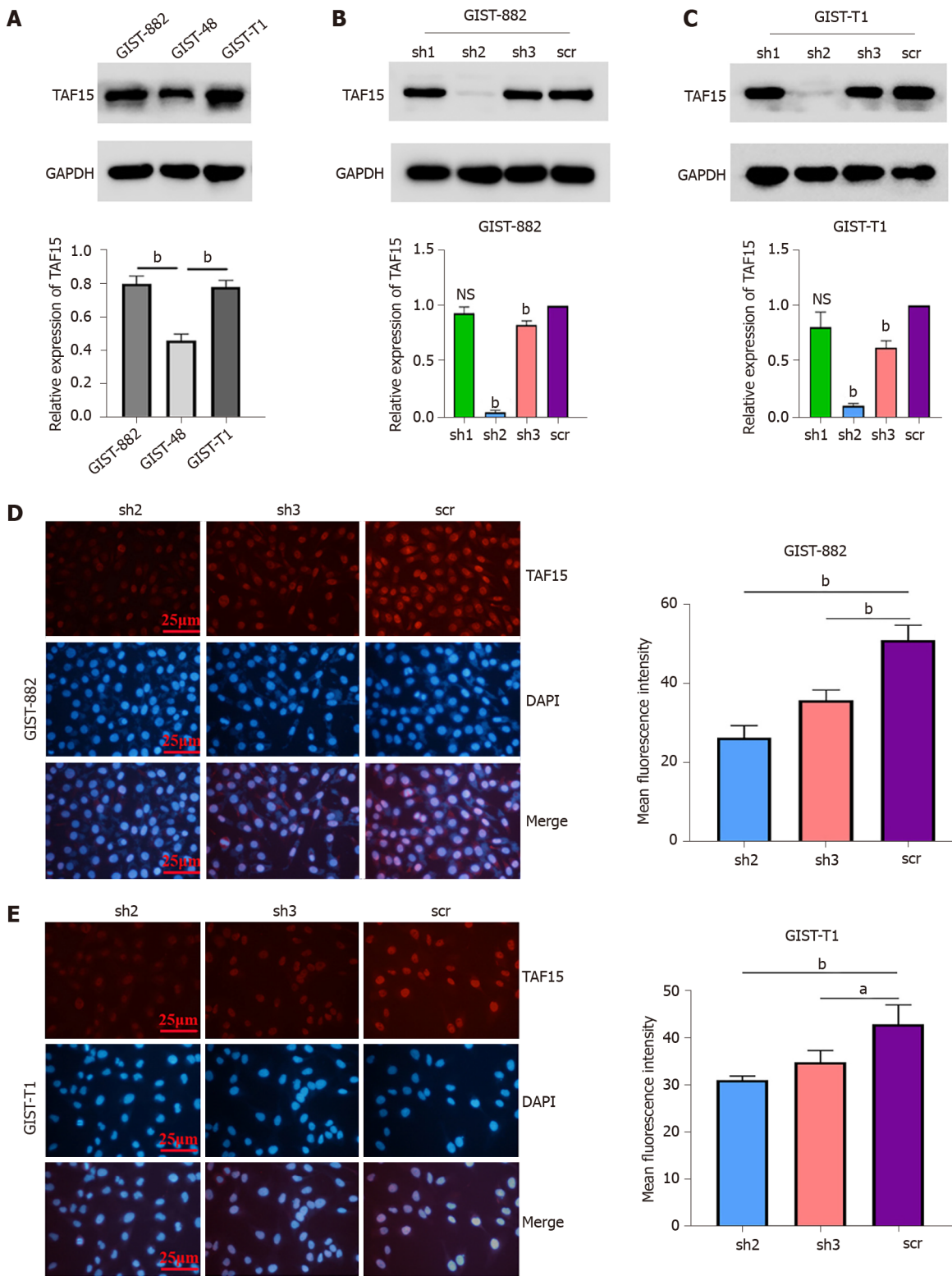
KIT and PDGFRA mutations are considered to be two major factors in GIST pathogenesis[3,26], and drugs targeting KIT and PDGFRA pathways have achieved great success in the treatment of this disease [27,28]. However, GIST patients gradually become resistant to current targeted drug treatment in recent years[14,28]. Therefore, there is an unmet need to explore other latent targets.

An increasing number of biomarkers or targets have been reported to be important to GIST progression. For example, p53 is a biomarker and potential target in GIST; targeting the p53 pathway is a novel additional treatment strategy for GIST[29]. High expression of carbohydrate antigen 125 is an independent risk factor for GIST progression, and it is a significant biomarker in the overall management of GIST patients[30]. Brain-derived neurotrophic factor is over expressed in high-risk GIST patients, and it may serve as a significant prognostic factor[31]. In the present study, proteomic analysis



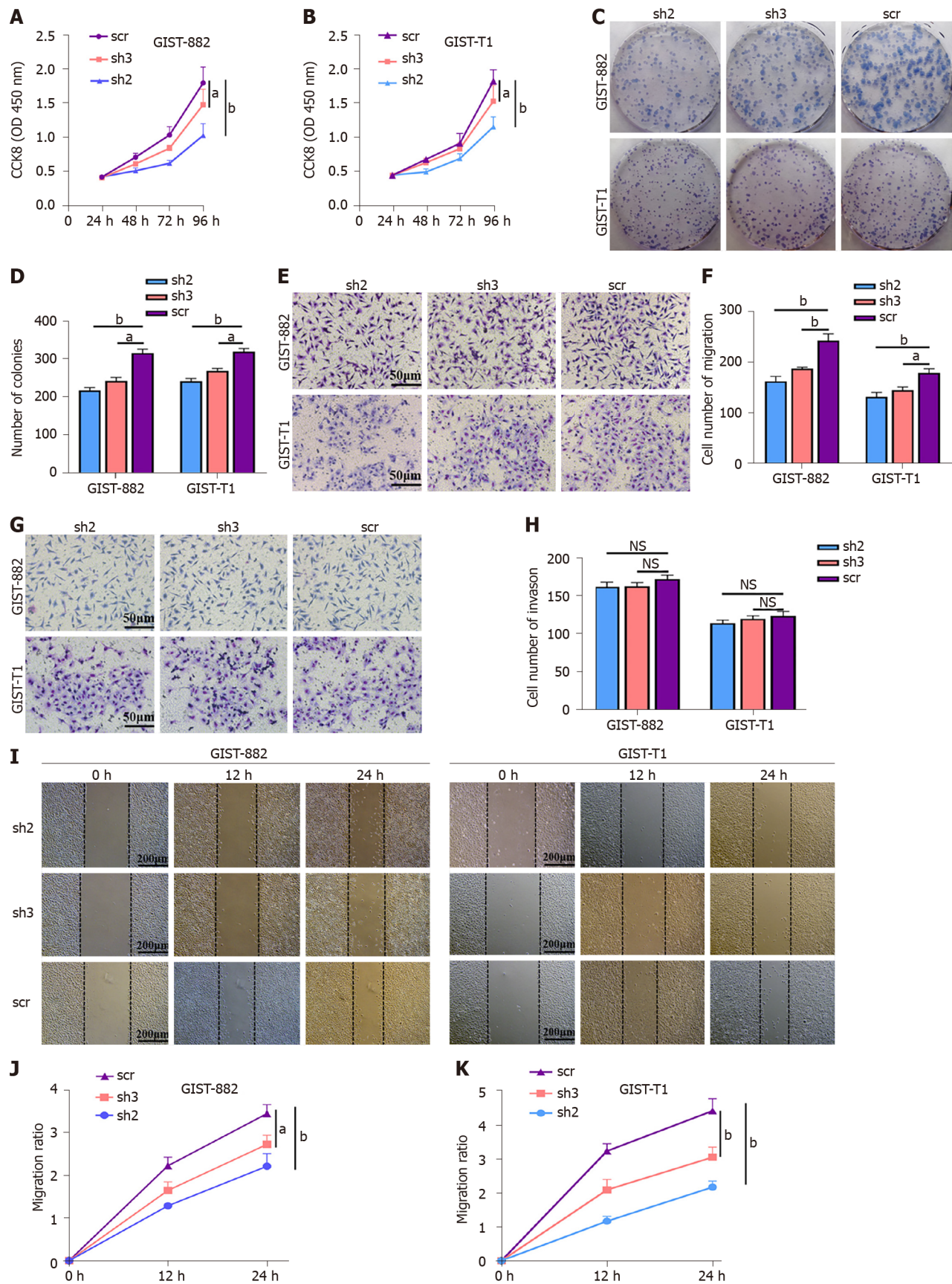
DOI: 10.3748/wjg.v29.i19.2932 Copyright ©The Author(s) 2023.

Figure 1 Differentially expressed proteins in gastrointestinal stromal tumor samples. A: Proteomic analysis identified the differentially expressed proteins in gastrointestinal stromal tumor (GIST) patients; B: Venn diagram showed the number of identified differentially expressed proteins in the subgroups of GIST; C and D: Western blotting identified that the expression level of TATA-box-binding protein-associated factor 15 (TAF15) was significantly increased in tumor tissues compared with matched normal tissues in all 18 GIST samples. *P* values were calculated using the Student's *t*-test; E: Immunohistochemical analysis verified the expression of TAF15 using 161 GIST tumor tissues and 18 matched normal tissues (representative images are shown and red arrows indicate positive staining); F: Total immunostaining score of TAF15 protein in tumor tissues and matched normal tissues of GIST; G: Total immunostaining score of TAF15 proteins in the GIST subgroup. *P* values were calculated using the Student's *t*-test or one-way analysis of variance. ^a*P* < 0.01. NS: No significance between groups; NIH-H: National Institutes of Health high risk; NIH-I: National Institutes of Health intermediate risk; NIH-L: National Institutes of Health low risk; NIH-VL: National Institutes of Health very low risk; IHC: Immunohistochemical; T: Tumor tissues; N: Normal tissues; FC: Fold change; TAF15: TATA-box-binding protein-associated factor 15.



DOI: 10.3748/wjg.v29.i19.2932 Copyright ©The Author(s) 2023.

Figure 2 The knockdown efficiency of short hairpin-TATA-box-binding protein-associated factor 15 in gastrointestinal stromal tumor cell lines. **A:** Western blotting to detect the expression level of TATA-box-binding protein-associated factor 15 (TAF15) in gastrointestinal stromal tumor(GIST) cell lines. *P* values were calculated by one-way analysis of variance; **B** and **C:** TAF15 was knocked down using three short hairpin (sh) RNAs (sh1, sh2, and sh3) and scrambled shRNA (scr) as control in GIST-882 and GIST-T1 cells. The results showed that sh2 and sh3 could reduce the expression level of TAF15 significantly when compared to scr as tested by western blotting analysis; **D** and **E:** The fluorescence intensity of TAF15 in sh2 and sh3 was reduced significantly when compared to scr in GIST-882 and GIST-T1 cells as tested by a cell immunofluorescence assay. *P* values were calculated using the Student's *t*-test. ^a*P* < 0.05, ^b*P* < 0.01. NS: No significance between groups; GIST: Gastrointestinal stromal tumor; TAF15: TATA-box-binding protein-associated factor 15; sh1: shRNA1 targeting TATA-box-binding protein-associated factor 15; sh2: shRNA2 targeting TATA-box-binding protein-associated factor 15; sh3: shRNA3 targeting TATA-box-binding protein-associated factor 15; scr: Scrambled shRNA.



DOI: 10.3748/wjg.v29.i19.2932 Copyright ©The Author(s) 2023.

Figure 3 TATA-box-binding protein-associated factor 15 regulated the proliferation and migration of gastrointestinal stromal tumor cells.

A and B: Cell counting kit-8 assay was performed to detect the proliferation of gastrointestinal stromal tumor (GIST)-882 and GIST-T1 after cell transfection. *P* values were calculated using the Student's *t*-test; C and D: A colony formation assay identified the proliferative ability of GIST-882 and GIST-T1 after cell transfection. Statistical analyses were performed using the Student's *t*-test; E-H: A transwell assay was performed to analyze the migratory and invasive ability of GIST-882 and

GIST-T1 cells after transfection. *P* values were calculated using the Student's *t*-test; I-K: A wound healing assay was conducted to confirm the migratory ability of GIST-882 and GIST-T1 cells after transfection. *P* values were calculated using the Student's *t*-test. ^a*P* < 0.05, ^b*P* < 0.01. GIST: Gastrointestinal stromal tumor; NS: No significance between groups; sh2: shRNA2 targeting TATA-box-binding protein-associated factor 15; sh3: shRNA3 targeting TATA-box-binding protein-associated factor 15; scr: Scrambled shRNA; CCK8: Cell counting kit-8.

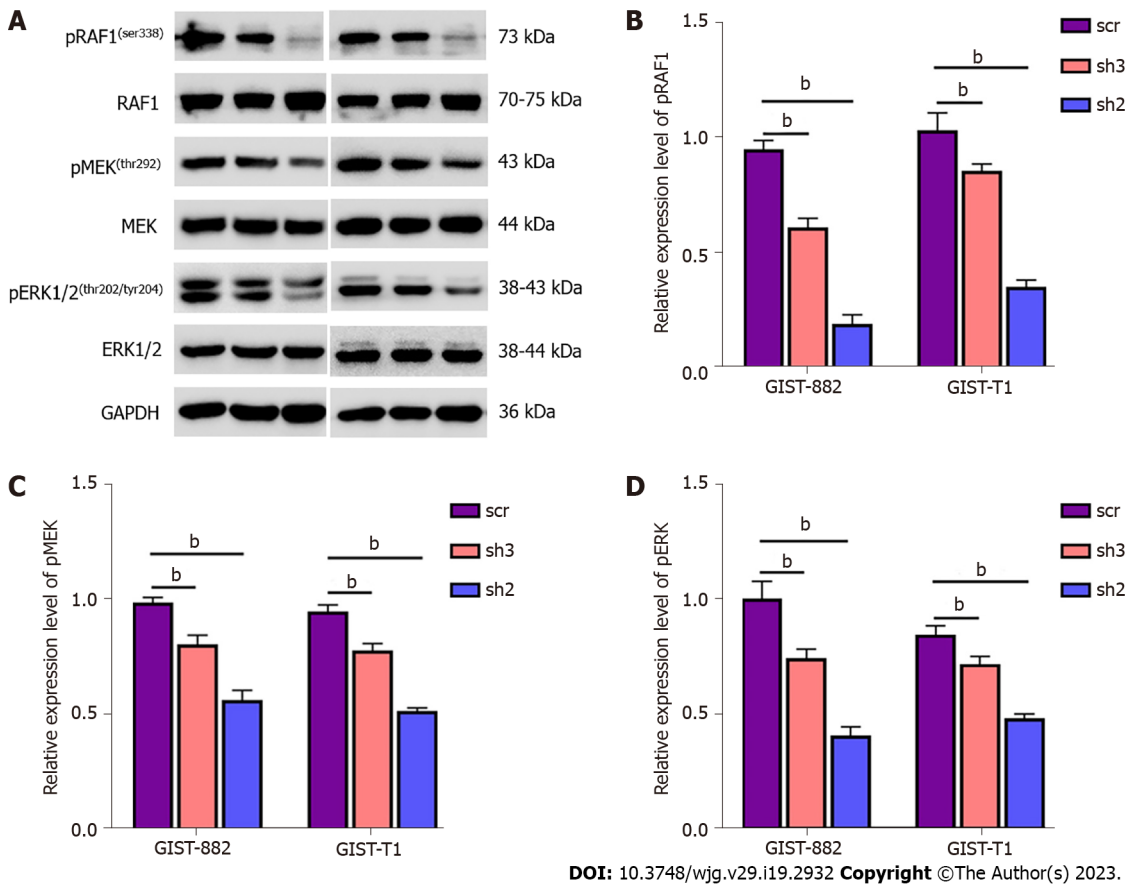


Figure 4 TATA-box-binding protein-associated factor 15 promoted the proliferation and migration of gastrointestinal stromal tumor cells by activating the RAF1/MEK/ERK pathway. A: Western blotting analysis detected the protein level of pRAF1/RAF1, pMEK/MEK and pERK/ERK in gastrointestinal stromal tumor (GIST)-882 and GIST-T1 after cell transfection; B-D: The phosphorylation levels of RAF1, MEK and ERK1/2 were significantly decreased in shRNA2 targeting TATA-box-binding protein-associated factor 15 and shRNA3 targeting TATA-box-binding protein-associated factor 15 when compared to the scrambled shRNA in GIST cell lines. Statistical analyses were executed by the Student's *t*-test. ^b*P* < 0.01. GIST: Gastrointestinal stromal tumor; sh2: shRNA2 targeting TATA-box-binding protein-associated factor 15; sh3: shRNA3 targeting TATA-box-binding protein-associated factor 15; scr: Scrambled shRNA.

was performed in patients with GIST to explore the potential molecular biomarkers for prediction, early diagnosis or treatment.

A total of 4111 quantified proteins with 1669 DEPs (762 upregulated and 907 downregulated proteins) were revealed in our study. Among the top 10 DEPs identified, TAF15 was interesting due to its key role in promoting growth in other human tumors such as extraskeletal myxoid sarcomas, leukemia, Ewing's sarcomas, human neuroblastoma and lung squamous cell carcinoma [15,17,19,20,32]. TAF15 was first reported as an RNA or DNA binding protein, while more recent studies have shown that TAF15 also plays important roles in cellular stress responses, cell spreading and cell adhesion [33,34]. GAS5 binding to TAF15 could upregulate expression of HIF1A, thus promoting wound healing in diabetic foot ulcers [35].

We believe our study is the first to confirm that TAF15 is over expressed in GIST tissues and cell lines and that high expression levels of TAF15 are positively correlated with tumor size and GIST risk stage. Previous studies have shown that the inhibition of TAF15 expression could significantly reduce cellular proliferation in melanoma and lung cancer [20,21]. Similarly, our study demonstrated that TAF15 knockdown could significantly inhibit proliferation and migration of GIST cells *in vitro* and suppress tumor growth *in vivo*. These data provided evidence that overexpression of TAF15 may contribute to the malignant progression of GIST.

The latent molecular mechanism of TAF15 in GIST was also first investigated in this study. Previous studies have shown that FET family proteins are mainly present in the nucleus [34], but it is now known that they also shuttle between the nucleus and cytoplasm [36-38]. They have an extensive functionality

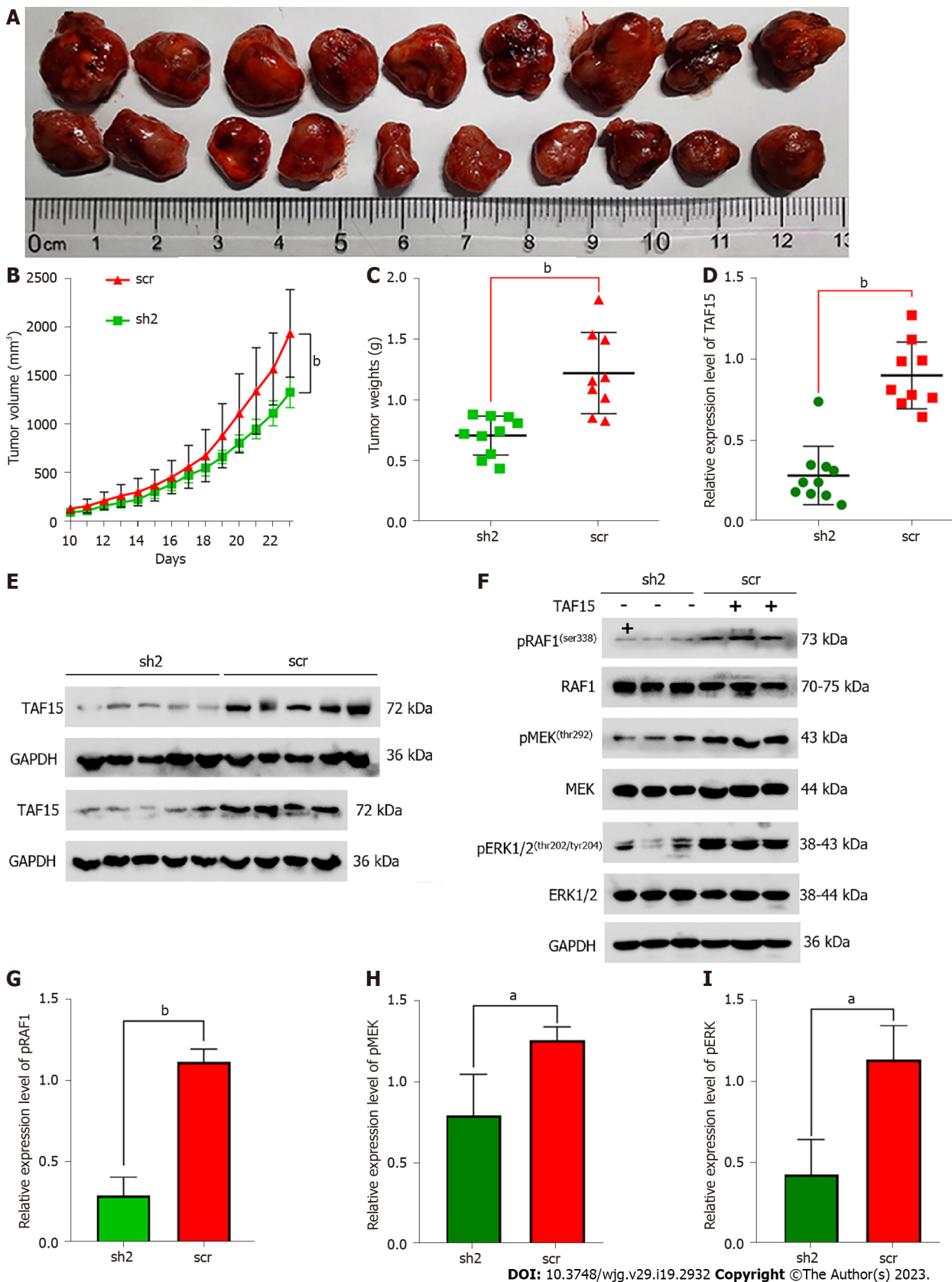


Figure 5 TATA-box-binding protein-associated factor 15 suppressed tumor growth of gastrointestinal stromal tumor cells *in vivo*. A-C: The volumes and weights of tumors in the shRNA2 targeting TATA-box-binding protein-associated factor 15 group were significantly smaller than the scrambled shRNA group. Statistical analyses were performed using the Student's *t*-test; D and E: Western blotting analysis was used to confirm the expression levels of TATA-box-binding protein-associated factor 15 in xenograft tumors; F-I: Western blotting analysis confirmed the protein levels of pRAF1/RAF1, pMEK/MEK and pERK/ERK in xenograft tumors. *P* values were calculated using the Student's *t*-test. ^a*P* < 0.05, ^b*P* < 0.01. TAF15: TATA-box-binding protein-associated factor 15; sh2: shRNA2 targeting TATA-box-binding protein-associated factor 15; scr: Scrambled shRNA.

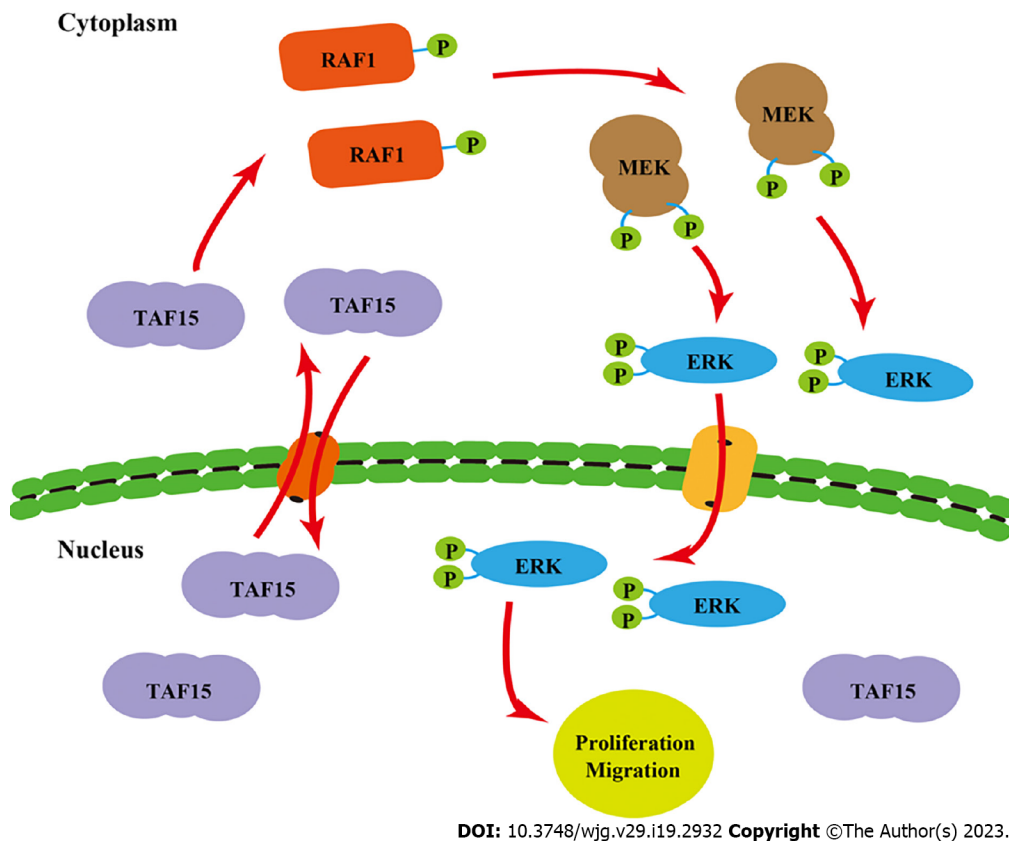


Figure 6 A schematic diagram of the mechanism of action of TATA-box-binding protein-associated factor 15 in gastrointestinal stromal tumors. TATA-box-binding protein-associated factor 15 shuttles between the nucleus and cytoplasm and promotes proliferation and migration of gastrointestinal stromal tumor cells by activating the RAF1/MEK/ERK pathway. TAF15: TATA-box-binding protein-associated factor 15.

including regulation and interaction with various proteins[39,40]. Moreover, recent work demonstrated that EWS-FLI1 fusion protein expression leads to activation of ERK1/2 signaling in zebrafish embryos and adult tumors[24]. Additionally, it is well known that the RAF/MEK/ERK signaling pathway plays an essential role in promoting cellular proliferation and survival[41].

In our study, we found TAF15 knockdown could significantly decrease the phosphorylation levels of RAF1, MEK and ERK, without significantly changing the total amounts of RAF1, MEK and ERK in GIST cell lines and xenograft tumors. Similarly, TAF15 is involved in the promotion of cell proliferation, migration and invasion of lung squamous cell carcinoma by activating the MAPK signaling pathway [22]. These results suggested that the activation of the ERK pathway may represent a new function of the TAF15 protein beyond DNA binding, mRNA splicing and mRNA transport. Taken together, these findings suggested that TAF15 shuttles between the nucleus and cytoplasm and may promote cell proliferation and migration directly through the activation of the RAF1/MEK/ERK signaling pathway in GIST (Figure 6). These observations greatly extend the functional repertoire of TAF15.

However, due to difficulty of obtaining matched tumor tissues after surgery[23], the number of paired samples used in this study for proteomic analysis, western blotting and IHC were small. Thus, we acknowledge that the accuracy of the proteomic analysis, western blotting and IHC in this research may be affected by the sample size and that the statistical analyses may be less robust due to the small sample size. Further studies will help validate some of the important and interesting findings of this study in larger GIST cohorts when available. Additional roles of TAF15 in GIST remain to be explored, as hundreds of genes lie downstream of TAF15[42].

CONCLUSION

In summary, this study utilized a proteomic analysis to find new molecular therapeutic targets for GIST and analyzed the expression level and underlying biological functions of TAF15 in GIST. Moreover, our study may be the first to demonstrate that TAF15 expression may contribute to malignant progression of GIST. TAF15 promoted cell proliferation and migration in GIST *via* the RAF1/MEK/ERK signaling pathway. Therefore, TAF15 is expected to be a novel latent molecular biomarker or therapeutic target of GIST.

ARTICLE HIGHLIGHTS

Research background

Gastrointestinal stromal tumors (GIST) are a common neoplasm with high rates of recurrence and metastasis, and its therapeutic efficacy is still not ideal. There is an unmet need to find new molecular therapeutic targets for GIST. TATA-box-binding protein-associated factor 15 (TAF15) contributes to the progress of various tumors, while the role and molecular mechanism of TAF15 in GIST progression are still unknown.

Research motivation

To explore the novel early diagnostic markers or therapeutic targets for the diagnosis and treatment of GIST.

Research objectives

To investigate new molecular therapeutic targets for GIST and explore the role and potential molecular mechanism of TAF15 in GIST progression.

Research methods

Proteomic analysis was performed to explore the differentially expressed proteins in GIST. Western blotting and immunohistochemical analysis were used to verify expression levels of TAF15 in GIST tissues and cell lines. Cell counting kit-8, colony formation, transwell, wound healing and western blotting assays were applied to explore the effect and the molecular mechanism of TAF15 in GIST. The role of TAF15 *in vivo* was confirmed using a xenograft mouse model assay.

Research results

A total of 1669 proteins were identified as differentially expressed proteins with 762 upregulated and 907 downregulated in GIST. TAF15 was significantly upregulated in GIST tissues and cell lines. Overexpression of TAF15 was associated with larger tumor size and higher risk stage of GIST. TAF15 knockdown suppressed proliferation and migration of GIST cells *in vitro* and inhibited the growth of GIST *in vivo*. Moreover, the inhibition of TAF15 expression significantly decreased the phosphorylation level of RAF1, MEK and ERK1/2 in GIST cells and xenograft tissues, while the total levels of RAF1, MEK and ERK1/2 had no significant changes.

Research conclusions

TAF15 may contribute to malignant progression of GIST and promote cell proliferation and migration in GIST *via* the activation of the RAF1/MEK/ERK signaling pathway.

Research perspectives

TAF15 is expected to be a novel latent molecular biomarker or therapeutic target of GIST.

FOOTNOTES

Author contributions: Guo CM and Tang L contributed equally to this work; Guo CM and Tang L performed the data acquisition, drafted the manuscript and executed the *in vitro* experiments; Guo CM completed the statistical analyses; Guo CM and Li X executed the animal experiments; Huang LY designed the work and revised the manuscript.

Supported by National Natural Science Foundation of China, No. 81870453.

Institutional review board statement: The study was conducted according to the guidelines of the Declaration of Helsinki, and approved by Ethics Committee of Yantai Yuhuangding Hospital, No. 2019-410.

Institutional animal care and use committee statement: All animal experiments were approved by the Affiliated Yantai Yuhuangding Hospital of Qingdao University for Laboratory Animal Welfare and Ethical Review, No. 2022-A56.

Informed consent statement: All study participants or their legal guardian provided informed written consent about personal and medical data collection prior to study enrolment.

Conflict-of-interest statement: All authors report having no relevant conflicts of interest for this article.

Data sharing statement: The data can be obtained from the corresponding author upon reasonable request.

ARRIVE guidelines statement: The authors have read the ARRIVE guidelines, and the manuscript was prepared and

revised according to the ARRIVE guidelines.

Open-Access: This article is an open-access article that was selected by an in-house editor and fully peer-reviewed by external reviewers. It is distributed in accordance with the Creative Commons Attribution NonCommercial (CC BY-NC 4.0) license, which permits others to distribute, remix, adapt, build upon this work non-commercially, and license their derivative works on different terms, provided the original work is properly cited and the use is non-commercial. See: <https://creativecommons.org/licenses/by-nc/4.0/>

Country/Territory of origin: China

ORCID number: Cheng-Ming Guo 0000-0002-6844-6223; Li Tang 0000-0002-1491-2129; Xu Li 0000-0002-4389-0352; Liu-Ye Huang 0000-0002-5016-0331.

S-Editor: Fan JR

L-Editor: Filipodia

P-Editor: Yu HG

REFERENCES

- 1 **Wu CE**, Tzen CY, Wang SY, Yeh CN. Clinical Diagnosis of Gastrointestinal Stromal Tumor (GIST): From the Molecular Genetic Point of View. *Cancers (Basel)* 2019; **11** [PMID: 31100836 DOI: 10.3390/cancers11050679]
- 2 **Casali PG**, Abecassis N, Aro HT, Bauer S, Biagini R, Bielack S, Bonvalot S, Boukovinas I, BoveeJVMG, Brodowicz T, Broto JM, Buonadonna A, De Álava E, Dei Tos AP, Del MuroXG, Dileo P, Eriksson M, Fedenko A, Ferraresi V, Ferrari A, Ferrari S, Frezza AM, Gasperoni S, Gelderblom H, Gil T, Grignani G, Gronchi A, Haas RL, Hassan B, Hohenberger P, Issels R, Joensuu H, Jones RL, Judson I, Jutte P, Kaal S, Kasper B, Kopeckova K, Krákorová DA, Le Cesne A, Lugowska I, Merimsky O, Montemurro M, Pantaleo MA, Piana R, Picci P, Piperno-Neumann S, Pousa AL, Reichardt P, Robinson MH, Rutkowski P, Safwat AA, Schöffski P, Sleijfer S, Stacchiotti S, Sundby Hall K, Unk M, Van Coevorden F, van der Graaf WTA, Whelan J, Wardelmann E, Zaikova O, Blay JY; ESMO Guidelines Committee and EURACAN. Gastrointestinal stromal tumours: ESMO-EURACAN Clinical Practice Guidelines for diagnosis, treatment and follow-up. *Ann Oncol* 2018; **29**: iv267 [PMID: 30188977 DOI: 10.1093/annonc/mdy320]
- 3 **Heinrich MC**, Corless CL, Duensing A, McGreevey L, Chen CJ, Joseph N, Singer S, Griffith DJ, Haley A, Town A, Demetri GD, Fletcher CD, Fletcher JA. PDGFRA activating mutations in gastrointestinal stromal tumors. *Science* 2003; **299**: 708-710 [PMID: 12522257 DOI: 10.1126/science.1079666]
- 4 **Miettinen M**, Lasota J. Gastrointestinal stromal tumors. *Gastroenterol Clin North Am* 2013; **42**: 399-415 [PMID: 23639648 DOI: 10.1016/j.gtc.2013.01.001]
- 5 **Xue A**, Gao X, He Y, Shu P, Huang X, Sun J, Lu J, Hou Y, Fang Y, Shen K. Role of Surgery in the Management of Liver Metastases From Gastrointestinal Stromal Tumors. *Front Oncol* 2022; **12**: 903487 [PMID: 35847933 DOI: 10.3389/fonc.2022.903487]
- 6 **Zhang D**, He C, Guo Y, Li J, Li B, Zhao Y, Yu L, Chang Z, Pei H, Yang M, Li N, Zhang Q, He Y, Pan Y, Zhao ZJ, Zhang C, Chen Y. Efficacy of SCF drug conjugate targeting c-KIT in gastrointestinal stromal tumor. *BMC Med* 2022; **20**: 257 [PMID: 35999600 DOI: 10.1186/s12916-022-02465-3]
- 7 **Joensuu H**, Vehtari A, Riihimäki J, Nishida T, Steigen SE, Brabec P, Plank L, Nilsson B, Cirilli C, Braconi C, Bordoni A, Magnusson MK, Linke Z, Sufliarsky J, Federico M, Jonasson JG, Dei Tos AP, Rutkowski P. Risk of recurrence of gastrointestinal stromal tumour after surgery: an analysis of pooled population-based cohorts. *Lancet Oncol* 2012; **13**: 265-274 [PMID: 22153892 DOI: 10.1016/S1470-2045(11)70299-6]
- 8 **Fletcher CD**, Berman JJ, Corless C, Gorstein F, Lasota J, Longley BJ, Miettinen M, O'Leary TJ, Remotti H, Rubin BP, Shmookler B, Sobin LH, Weiss SW. Diagnosis of gastrointestinal stromal tumors: A consensus approach. *Hum Pathol* 2002; **33**: 459-465 [PMID: 12094370 DOI: 10.1053/hupa.2002.123545]
- 9 **Li S**, Chen D, Li S, Zhao Z, Yang H, Wang D, Zhang Z, Fu W. Novel Prognostic Nomogram for Recurrence-Free Survival of Patients With Primary Gastrointestinal Stromal Tumors After Surgical Resection: Combination of Prognostic Nutritional Index and Basic Variables. *Front Oncol* 2020; **10**: 581855 [PMID: 33585198 DOI: 10.3389/fonc.2020.581855]
- 10 **Bang YH**, Ryu MH, Kim HD, Lee HE, Kang YK. Clinical outcomes and prognostic factors for patients with high-risk gastrointestinal stromal tumors treated with 3-year adjuvant imatinib. *Int J Cancer* 2022; **151**: 1770-1777 [PMID: 35678337 DOI: 10.1002/ijc.34157]
- 11 **Nunobe S**, Sano T, Shimada K, Sakamoto Y, Kosuge T. Surgery including liver resection for metastatic gastrointestinal stromal tumors or gastrointestinal leiomyosarcomas. *Jpn J Clin Oncol* 2005; **35**: 338-341 [PMID: 15928191 DOI: 10.1093/jjco/hyi091]
- 12 **Keung EZ**, Raut CP, Rutkowski P. The Landmark Series: Systemic Therapy for Resectable Gastrointestinal Stromal Tumors. *Ann Surg Oncol* 2020; **27**: 3659-3671 [PMID: 32734368 DOI: 10.1245/s10434-020-08869-w]
- 13 **Hemming ML**, Heinrich MC, Bauer S, George S. Translational insights into gastrointestinal stromal tumor and current clinical advances. *Ann Oncol* 2018; **29**: 2037-2045 [PMID: 30101284 DOI: 10.1093/annonc/mdy309]
- 14 **Joensuu H**, Rutkowski P, Nishida T, Steigen SE, Brabec P, Plank L, Nilsson B, Braconi C, Bordoni A, Magnusson MK, Sufliarsky J, Federico M, Jonasson JG, Hostein I, Bringuier PP, Emile JF. KIT and PDGFRA mutations and the risk of GI stromal tumor recurrence. *J Clin Oncol* 2015; **33**: 634-642 [PMID: 25605837 DOI: 10.1200/JCO.2014.57.4970]
- 15 **Lindén M**, Vannas C, Österlund T, Andersson L, Osman A, Escobar M, Fagman H, Ståhlberg A, Åman P. FET fusion oncoproteins interact with BRD4 and SWI/SNF chromatin remodelling complex subtypes in sarcoma. *Mol Oncol* 2022;

- 16: 2470-2495 [PMID: 35182012 DOI: 10.1002/1878-0261.13195]
- 16 **Glisovic T**, Bachorik JL, Yong J, Dreyfuss G. RNA-binding proteins and post-transcriptional gene regulation. *FEBS Lett* 2008; **582**: 1977-1986 [PMID: 18342629 DOI: 10.1016/j.febslet.2008.03.004]
 - 17 **Zuo L**, Zhang G, Massett M, Cheng J, Guo Z, Wang L, Gao Y, Li R, Huang X, Li P, Qi Z. Loci-specific phase separation of FET fusion oncoproteins promotes gene transcription. *Nat Commun* 2021; **12**: 1491 [PMID: 33674598 DOI: 10.1038/s41467-021-21690-7]
 - 18 **Wang J**, Cai Y, Lu H, Zhang F, Zheng J. LncRNA APOA1-AS facilitates proliferation and migration and represses apoptosis of VSMCs through TAF15-mediated SMAD3 mRNA stabilization. *Cell Cycle* 2021; **20**: 1642-1652 [PMID: 34382908 DOI: 10.1080/15384101.2021.1951940]
 - 19 **Ballarino M**, Jobert L, Dembélé D, de la Grange P, Auboeuf D, Tora L. TAF15 is important for cellular proliferation and regulates the expression of a subset of cell cycle genes through miRNAs. *Oncogene* 2013; **32**: 4646-4655 [PMID: 23128393 DOI: 10.1038/onc.2012.490]
 - 20 **Singh AK**, Kapoor V, Thotala D, Hallahan DE. TAF15 contributes to the radiation-inducible stress response in cancer. *Oncotarget* 2020; **11**: 2647-2659 [PMID: 32676166 DOI: 10.18632/oncotarget.27663]
 - 21 **Schatz N**, Brändlein S, Rückl K, Hensel F, Vollmers HP. Diagnostic and therapeutic potential of a human antibody cloned from a cancer patient that binds to a tumor-specific variant of transcription factor TAF15. *Cancer Res* 2010; **70**: 398-408 [PMID: 20048082 DOI: 10.1158/0008-5472.CAN-09-2186]
 - 22 **Zhu H**, Liu Q, Yang X, Ding C, Wang Q, Xiong Y. LncRNA LINC00649 recruits TAF15 and enhances MAPK6 expression to promote the development of lung squamous cell carcinoma via activating MAPK signaling pathway. *Cancer Gene Ther* 2022; **29**: 1285-1295 [PMID: 35228660 DOI: 10.1038/s41417-021-00410-9]
 - 23 **Li J**, Ye Y, Wang J, Zhang B, Qin S, Shi Y, He Y, Liang X, Liu X, Zhou Y, Wu X, Zhang X, Wang M, Gao Z, Lin T, Cao H, Shen L; Chinese Society Of Clinical Oncology CSCO Expert Committee On Gastrointestinal Stromal Tumor. Chinese consensus guidelines for diagnosis and management of gastrointestinal stromal tumor. *Chin J Cancer Res* 2017; **29**: 281-293 [PMID: 28947860 DOI: 10.21147/j.issn.1000-9604.2017.04.01]
 - 24 **Vasileva E**, Warren M, Triche TJ, Amatruda JF. Dysregulated heparan sulfate proteoglycan metabolism promotes Ewing sarcoma tumor growth. *Elife* 2022; **11** [PMID: 35285802 DOI: 10.7554/eLife.69734]
 - 25 **Ullah R**, Yin Q, Snell AH, Wan L. RAF-MEK-ERK pathway in cancer evolution and treatment. *Semin Cancer Biol* 2022; **85**: 123-154 [PMID: 33992782 DOI: 10.1016/j.semcancer.2021.05.010]
 - 26 **Miettinen M**, Sarlomo-Rikala M, Lasota J. Gastrointestinal stromal tumors: recent advances in understanding of their biology. *Hum Pathol* 1999; **30**: 1213-1220 [PMID: 10534170 DOI: 10.1016/s0046-8177(99)90040-0]
 - 27 **Serrano C**, Mariño-Enríquez A, Tao DL, Ketzler J, Eilers G, Zhu M, Yu C, Mannan AM, Rubin BP, Demetri GD, Raut CP, Presnell A, McKinley A, Heinrich MC, Czaplinski JT, Sicinska E, Bauer S, George S, Fletcher JA. Complementary activity of tyrosine kinase inhibitors against secondary kit mutations in imatinib-resistant gastrointestinal stromal tumours. *Br J Cancer* 2019; **120**: 612-620 [PMID: 30792533 DOI: 10.1038/s41416-019-0389-6]
 - 28 **Demetri GD**, Reichardt P, Kang YK, Blay JY, Rutkowski P, Gelderblom H, Hohenberger P, Leahy M, von Mehren M, Joensuu H, Badalamenti G, Blackstein M, Le Cesne A, Schöffski P, Maki RG, Bauer S, Nguyen BB, Xu J, Nishida T, Chung J, Kappeler C, Kuss I, Laurent D, Casali PG; GRID study investigators. Efficacy and safety of regorafenib for advanced gastrointestinal stromal tumours after failure of imatinib and sunitinib (GRID): an international, multicentre, randomised, placebo-controlled, phase 3 trial. *Lancet* 2013; **381**: 295-302 [PMID: 23177515 DOI: 10.1016/S0140-6736(12)61857-1]
 - 29 **Wu CE**, Chen CP, Huang WK, Pan YR, Aptullahoglu E, Yeh CN, Lunec J. p53 as a biomarker and potential target in gastrointestinal stromal tumors. *Front Oncol* 2022; **12**: 872202 [PMID: 35965531 DOI: 10.3389/fonc.2022.872202]
 - 30 **Sui C**, Lin C, Tao T, Guan W, Zhang H, Tao L, Wang M, Wang F. Prognostic significance of serum CA125 in the overall management for patients with gastrointestinal stromal tumors. *BMC Gastroenterol* 2023; **23**: 25 [PMID: 36703123 DOI: 10.1186/s12876-023-02655-0]
 - 31 **Tian GA**, Xu WT, Sun Y, Wang J, Ke Q, Yuan MJ, Wang JJ, Zhuang C, Gong Q. BDNF expression in GISTs predicts poor prognosis when associated with PD-L1 positive tumor-infiltrating lymphocytes. *Oncoimmunology* 2021; **10**: 2003956 [PMID: 34804639 DOI: 10.1080/2162402X.2021.2003956]
 - 32 **Xiong Y**, Yang C, Yang X, Ding C, Wang Q, Zhu H. LncRNA MIR9-3HG enhances LIMK1 mRNA and protein levels to contribute to the carcinogenesis of lung squamous cell carcinoma via sponging miR-138-5p and recruiting TAF15. *Pathol Res Pract* 2022; **237**: 153941 [PMID: 35933883 DOI: 10.1016/j.prp.2022.153941]
 - 33 **de Hoog CL**, Foster LJ, Mann M. RNA and RNA binding proteins participate in early stages of cell spreading through spreading initiation centers. *Cell* 2004; **117**: 649-662 [PMID: 15163412 DOI: 10.1016/s0092-8674(04)00456-8]
 - 34 **Andersson MK**, Ståhlberg A, Arvidsson Y, Olofsson A, Semb H, Stenman G, Nilsson O, Aman P. The multifunctional FUS, EWS and TAF15 proto-oncoproteins show cell type-specific expression patterns and involvement in cell spreading and stress response. *BMC Cell Biol* 2008; **9**: 37 [PMID: 18620564 DOI: 10.1186/1471-2121-9-37]
 - 35 **Peng WX**, He PX, Liu LJ, Zhu T, Zhong YQ, Xiang L, Peng K, Yang JJ, Xiang GD. LncRNA GAS5 activates the HIF1A/VEGF pathway by binding to TAF15 to promote wound healing in diabetic foot ulcers. *Lab Invest* 2021; **101**: 1071-1083 [PMID: 33875793 DOI: 10.1038/s41374-021-00598-2]
 - 36 **Marko M**, Vlassis A, Guialis A, Leichter M. Domains involved in TAF15 subcellular localisation: dependence on cell type and ongoing transcription. *Gene* 2012; **506**: 331-338 [PMID: 22771914 DOI: 10.1016/j.gene.2012.06.088]
 - 37 **Zinszner H**, Sok J, Immanuel D, Yin Y, Ron D. TLS (FUS) binds RNA *in vivo* and engages in nucleocytoplasmic shuttling. *J Cell Sci* 1997; **110** (Pt 15): 1741-1750 [PMID: 9264461 DOI: 10.1242/jcs.110.15.1741]
 - 38 **Zakaryan RP**, Gehring H. Identification and characterization of the nuclear localization/retention signal in the EWS proto-oncoprotein. *J Mol Biol* 2006; **363**: 27-38 [PMID: 16965792 DOI: 10.1016/j.jmb.2006.08.018]
 - 39 **Law WJ**, Cann KL, Hicks GG. TLS, EWS and TAF15: a model for transcriptional integration of gene expression. *Brief Funct Genomic Proteomic* 2006; **5**: 8-14 [PMID: 16769671 DOI: 10.1093/bfpg/ell015]
 - 40 **Rual JF**, Venkatesan K, Hao T, Hirozane-Kishikawa T, Dricot A, Li N, Berriz GF, Gibbons FD, Dreze M, Ayivi-

Guedehoussou N, Klitgord N, Simon C, Boxem M, Milstein S, Rosenberg J, Goldberg DS, Zhang LV, Wong SL, Franklin G, Li S, Albala JS, Lim J, Fraughton C, Llamosas E, Cevik S, Bex C, Lamesch P, Sikorski RS, Vandenhoute J, Zoghbi HY, Smolyar A, Bosak S, Sequerra R, Doucette-Stamm L, Cusick ME, Hill DE, Roth FP, Vidal M. Towards a proteome-scale map of the human protein-protein interaction network. *Nature* 2005; **437**: 1173-1178 [PMID: [16189514](#) DOI: [10.1038/nature04209](#)]

- 41 **Yaeger R**, Corcoran RB. Targeting Alterations in the RAF-MEK Pathway. *Cancer Discov* 2019; **9**: 329-341 [PMID: [30770389](#) DOI: [10.1158/2159-8290.CD-18-1321](#)]
- 42 **Kume K**, Ikeda M, Miura S, Ito K, Sato KA, Ohmori Y, Endo F, Katagiri H, Ishida K, Ito C, Iwaya T, Nishizuka SS. α -Amanitin Restrains Cancer Relapse from Drug-Tolerant Cell Subpopulations *via* TAF15. *Sci Rep* 2016; **6**: 25895 [PMID: [27181033](#) DOI: [10.1038/srep25895](#)]



Published by **Baishideng Publishing Group Inc**
7041 Koll Center Parkway, Suite 160, Pleasanton, CA 94566, USA
Telephone: +1-925-3991568
E-mail: bpgoffice@wjgnet.com
Help Desk: <https://www.f6publishing.com/helpdesk>
<https://www.wjgnet.com>

